ChemComm

COMMUNICATION

View Article Online
View Journal | View Issue

Cite this: *Chem. Commun.*, 2015, 51, 772

Received 13th October 2014,
Accepted 20th November 2014

DOI: 10.1039/c4cc08086f

www.rsc.org/chemcomm

Glycan reductive isotope-coded amino acid labeling (GRIAL) for mass spectrometry-based quantitative *N*-glycomics†

Yan Cai,[ab] Jing Jiao,[ab] Zhichao Bin,[b] Ying Zhang,*[ab] Pengyuan Yang[b] and Haojie Lu*[ab]

A general and simple labeling method, termed glycan reductive isotope-coded amino acid labeling (GRIAL), was developed for mass spectrometry-based quantitative *N*-glycomics.

N-glycosylation is the most common and most complex post-translational modification of proteins. Aberrant *N*-glycosylation is associated with a variety of human diseases, such as tumor progression, immune deficiencies, and inflammation.[1] Therefore, quantitative analysis of total *N*-glycan profiles can provide insight into glycan functions in biological processes and disease development.

In the past decade, mass spectrometry (MS)-based stable isotopic labeling has become a powerful tool for the qualitative profiling of *N*-glycome.[2] Currently, enzymatic ^{18}O-labeling, metabolic labeling, and chemical labeling are the three main approaches. In the enzymatic ^{18}O-labeling approach,[3] *N*-glycans are released from glycoproteins by endoglycosidase in the presence of ^{18}O-water to incorporate ^{18}O into the reducing ends of glycans. However, the isotope overlap caused by only 2 Da mass difference between ^{16}O- and ^{18}O-labeled glycans requires an extra deconvolution step to achieve accurate quantitation. In addition, endoglycosidases are not comprehensive as peptide-*N*-glycosidase F (PNGase F) for glycan release, making this method less desirable. Metabolic labeling is an alternative approach for glycan quantitation, which takes advantage of the biosynthetic pathways of hexosamine. In the isotopic detection of amino sugars using the glutamine (IDAWG) strategy,[4] labeled samples are mixed together at the cell culture stage, and variations in sample preparation are minimized. However, the critical drawback of this IDAWG strategy is that it is just limited to the investigation of cultured cell systems and cannot be extended to serum or tissue samples. Compared with enzymatic ^{18}O labeling and metabolic labeling, chemical labeling based on the reaction at the terminal aldehyde-group of glycans is more prevalent, as it is versatile and the origin of samples can be biologically different. A few isotope-coded reagents, such as 2-aminopyridine (2-AP),[5] 2-aminobenzoic acid (2-AA),[6] aniline,[7] and 4-phenethylbenzohydrazide (P2GPN),[8] have been demonstrated to be effective in the quantitative analysis of glycans. However, these isotope-coded reagents are commonly limited to two samples in a single analysis. Recently, tetraplex aniline tags (D_0, D_4, D_8, and D_{12}) were synthesized, allowing multiplexed quantitation of four samples simultaneously, but the deuterium isotopes may cause chromatographic isotope effects.[9] Additionally, the use of isobaric aldehyde reactive tags (iARTs)[10] and stable isotope labeled carbonyl-reactive tandem mass tags (Glyco-TMTs)[11] was explored as a novel approach for quantitation of glycans in the tandem mass spectrum, respectively. Although isotope labeling at the reducing ends of glycans has shed light on quantitative *N*-glycomics, the in-house design, synthesis and characterization of these specific isotope-coded reagents are very tedious and time-consuming, making them inevitably less popular among different laboratories.

Isotope-coded amino acids are commercially available reagents for MS-based quantitative proteomics.[12] Recently, a novel approach for identification and quantitation of C-terminal peptides *via* incorporation of an isotopic arginine based on oxazolone chemistry was reported.[13] Herein, isotope-coded amino acids were used to quantify *N*-glycans, where the reducing end of a *N*-glycan was labeled with isotope-coded arginine at the side chain NH_2 group through reductive amination (Scheme 1).[14]

The GRIAL strategy offers the following advantages for quantitative analysis of *N*-glycans by MS. First, the labeling efficiency of the GRIAL strategy was determined to be almost 100%. As shown in Fig. 1A, native DP7 was detected as $[M + Na]^+$ and $[M + K]^+$ at *m*/*z* 1175.28 and 1191.25, respectively. After labeling with Arg($^{12}C_6$), $[M + Arg^0 + H]^+$ and $[M + Arg^0 + Na]^+$ at *m*/*z* 1311.46 and 1333.43 were detected with the predicted mass shift of 158 Da. No signals of native DP7 were observed, indicating the nearly 100% labeling efficiency of the GRIAL strategy (Fig. 1B).

[a] *Shanghai Cancer Center and Key Laboratory of Glycoconjugates Research Ministry of Public Health, Fudan University, Shanghai 200032, P. R. China. E-mail: ying@fudan.edu.cn, luhaojie@fudan.edu.cn; Fax: +86 21 54237961; Tel: +86 21 54237618*

[b] *Institutes of Biomedical Sciences and Department of Chemistry, Fudan University, Shanghai, 200032, P. R. China*

† Electronic supplementary information (ESI) available. See DOI: 10.1039/c4cc08086f

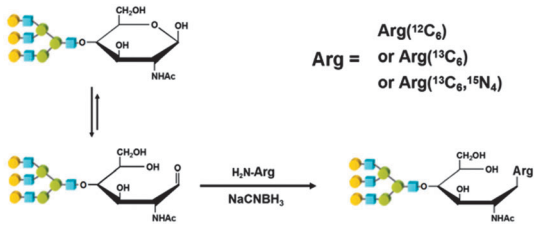

Scheme 1 GRIAL strategy using Arg by the reductive amination reaction.

After labeling with Arg($^{13}C_6$), similar results were obtained with a mass shift of 164 Da (Fig. S1A, ESI†). The nearly 100% labeling efficiency was further confirmed by analysis of the mixture of native DP7 and Arg($^{12}C_6$) labeled DP7 in molar ratios of 1 : 5 and 1 : 10, because the S/N ratio of native DP7 did not increase as more labeled DP7 was mixed (Fig. S1B and C, ESI†). To demonstrate the feasibility of the GRIAL strategy in a more complex mixture, *N*-glycans released from two model glycoproteins were labeled with Arg($^{12}C_6$) and Arg($^{13}C_6$). As shown in Fig. S2 and S3 (ESI†), *N*-glycans from both RNase B and OVA were completely converted into their corresponding $[M + Arg^0 + H]^+$ form or $[M + Arg^6 + H]^+$ form, which demonstrated that the GRIAL strategy is a general method with high labeling efficiency for further glycan quantitation.

The second advantage of the GRIAL strategy is that it can improve the signal-to-noise (S/N) ratios of glycans. As we know, a higher S/N ratio can facilitate quantitation, but analysis of native glycans by MS is often limited by their low ionization efficiency. As illustrated in Fig. 1C, the S/N ratio of Arg($^{12}C_6$) labeled DP7 (*m*/*z* 1311.52) was approximately 3.6-fold higher than that of native DP7 (*m*/*z* 1175.37). For a complex mixture of glycans, such as Dextran 1000, it was also found that the S/N ratios of labeled glycans were increased by approximately 3.7–5.5-fold (Fig. S4, ESI†). These results indicated that the GRIAL strategy is very useful for improved analysis of glycans by MS.

The third advantage is that the use of Arg($^{13}C_6$) in the GRIAL strategy causes no chromatographic isotope effects compared to deuterium encoded tags. As shown in Fig. S5 (ESI†), DP7 labeled with Arg($^{12}C_6$) and DP7 labeled with Arg($^{13}C_6$) were coeluted at a retention time of 2.99 min during HILIC-MS analysis, indicating that there were no chromatographic isotope effects using isotope-coded arginines.

The fourth advantage of the GRIAL strategy is described as follows: compared with the enzymatic ^{18}O labeling approach, the GRIAL strategy offered a larger mass difference of 6 Da, avoiding inaccurate glycan quantitation due to isotope interference. Additionally, compared with the homemade isotopic tags, the GRIAL strategy could be readily extended to three-plex tags for glycan quantitation because of the commercial availability of another isotope-coded arginine, Arg^{10}($^{13}C_6$, $^{15}N_4$), and this feature will make this novel strategy easily accessible by other laboratories.

Using the GRIAL strategy, *N*-glycans from multiple samples were relatively quantitated. Relative *N*-glycan quantitation was obtained by comparison of ion abundance of light and heavy arginine labeled samples (in terms of signal intensity of a monoisotopic peak). The accuracy, reproducibility and dynamic range of the GRIAL strategy for glycan quantitation were evaluated. Fig. S6 (ESI†) illustrates the mass spectra of the mixture of Arg($^{12}C_6$) and Arg($^{13}C_6$) labeled DP7 in molar ratios of 1 : 1, 1 : 5 and 1 : 10. A series of 6 Da difference doublets of Arg($^{12}C_6$) and Arg($^{13}C_6$) labeled DP7 were observed and the measured ratios were consistent with the theoretical ratios. Dual-logarithm plots of the theoretical ratios *vs.* the measured ratios were generated, exhibiting a good coefficient of variation (CV) ranging from 1.3 to 9.2% and a high correlation coefficient (R^2 = 0.9984) within 2 orders of magnitude within the dynamic range (Fig. 2). Subsequently, a model glycan NA2 with complex structure, *N*-glycans with high mannose structure from RNase B and *N*-glycans with hybrid structure from OVA were labeled with Arg($^{12}C_6$) and Arg($^{13}C_6$), respectively. As shown in Fig. S7 (ESI†), a series of 6 Da difference doublets for each glycan were also detected. For NA2 and Man 5, Man 6, and Man 8 from RNase B, quantitative results are illustrated in Fig. S8 (ESI†). The above results demonstrated that the GRIAL strategy could also provide a good linearity ($R^2 > 0.99$) and a high reproducibility (CV < 18.1%) within 2 orders of magnitude in the dynamic range for complex samples.

The fifth advantage of the GRIAL strategy is that enhanced S/N ratios of tandem MS fragmentation ions and a simplified tandem spectrum are obtained for structural deduction, and

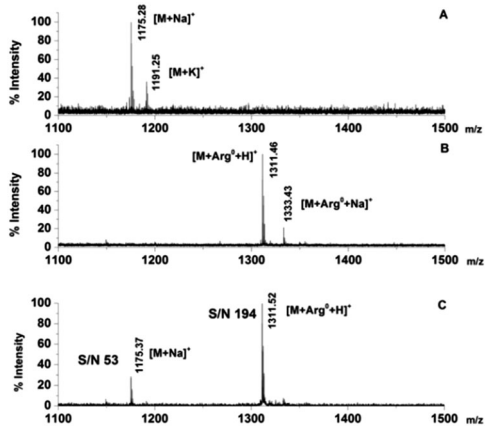

Fig. 1 MALDI-TOF mass spectra of (A) native DP7, (B) DP7 labeled with Arg($^{12}C_6$), and (C) an equimolar mixture of native DP7 and DP7 labeled with Arg($^{12}C_6$).

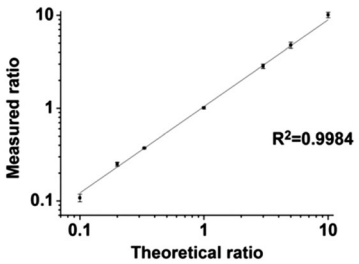

Fig. 2 Dynamic range and accuracy of quantitation of the model glycan. DP7 labeled with Arg($^{12}C_6$) and Arg($^{13}C_6$) were mixed in known molar ratios (1 : 10, 1 : 5, 1 : 3, 1 : 1, 3 : 1, 5 : 1, and 10 : 1), and each experiment was repeated three times.

the generated consecutive Y-type ions can be used for discriminating isomeric glycans. Fragmentation of the same amount of native DP7 $[M + Na]^+$ (10 pmol) was chosen as a control. As shown in Fig. S9A (ESI†) top, for native DP7 $[M + Na]^+$ at *m/z* 1175.40 as the precursor ion, glycosidic cleavages produced both Y-type ions and B-type ions with low S/N ratios in the tandem mass spectrum, making it difficult to assign them to a particular fragment of a given glycan. In contrast, after labeling with Arg($^{12}C_6$), for the corresponding precursor ion $[M + Arg^0 + H]^+$ (*m/z* 1311.46) or $[M + Arg^6 + H]^+$ (*m/z* 1317.44), a series of consecutive Y-type ions (Y_1–Y_6 and Y_1*–Y_6*) was predominately observed with improved S/N ratios (2–10-fold) in the tandem mass spectrum (Fig. S9A (ESI†), middle and bottom). This can be explained by the fact that, using the GRIAL strategy, the charge is localized at the labeled reducing terminus of the precursor during the fragmentation due to the proton affinity of arginine, so Y-type ions are preferably formed.[15] Therefore, the sequence of an unknown glycan could be easily deduced from the simplified tandem mass spectrum. To verify the ability of the GRIAL strategy to discriminate isomeric glycans, a pair of glycan isomers at *m/z* 1663.59 from two different glycoproteins was analyzed. One from OVA is a hybrid-type glycan, and the other from ASF is a complex-type glycan. Fig. S9B (ESI†) displays the MS/MS fragmentation of the corresponding precursor at *m/z* 1799.54. The fragment ion $Y_{3\beta}$ at *m/z* 1313.93 and $Y_{3\gamma}$ at *m/z* 1596.55 only appeared in Fig. S9B (ESI†) top, indicating that the corresponding precursor was the hybrid glycan from OVA. Meanwhile, the fragment ion Y_3 at *m/z* 1272.44 only appeared in Fig. S9B (ESI†) bottom, indicating that the corresponding precursor was the complex glycan from ASF.

To test the application of the GRIAL strategy in real biological samples, the quantitative analysis of serum *N*-glycans from healthy control and CRC patients was performed. Native DP7 was used as the spiked standard before labeling. As shown in Fig. S10 (ESI†), a total of 31 glycan pairs in both normal and CRC serum were detected. Table S1 (ESI†) illustrates their glycoforms, CRC/normal ratios and CVs. The CVs of CRC/normal ratios varied from 1.3% to 28.5% in triplicate analysis. Because the CVs were no more than 30%, the CRC/normal ratio >1.30 or <0.77 was regarded as a criterion for definite changes in the levels of glycosylation. From Fig. 3, it could be concluded that 13 glycans were up-regulated in the CRC serum, most of them presenting the complex and bisecting structure. Additionally, among these highly expressed glycans, 4 glycans were core-fucosylated and 2 glycans were sialylated. These results are in accordance with previous findings that the increased degree of branching in *N*-glycans and elevated levels of sialylation and core-fucosylation played a critical role in CRC progression.[16] Therefore, the GRIAL strategy is suitable for quantitative analysis of the complex *N*-glycome.

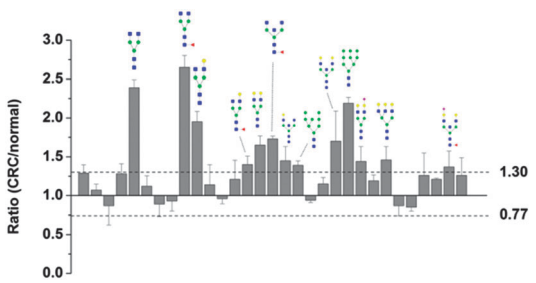

Fig. 3 Relative quantitation of *N*-glycans from normal and CRC human serum (n = 3). A CRC/normal ratio <0.77 or >1.30 is regarded as a criterion to estimate down- or up-regulation of the glycan abundance.

In this work, we developed isotope-coded amino acids as novel tags *via* reductive amination for *N*-glycan quantitation. Due to readily available isotope-coded amino acids as commercial reagents, GRIAL has great potential to be accessible to most laboratories. The GRIAL for glycans is complete (almost 100%) and can enhance the ionization efficiency (3.6–5.5-fold). GRIAL shows a good linearity ($R^2 > 0.99$) and a high reproducibility (CV $< 18.1\%$) within 2 orders of magnitude in the dynamic range. Additionally, tandem mass spectra of labeled *N*-glycans show simplified fragmentation, facilitating the interpretation of the spectra for glycan identification and the discrimination of glycan isomers.

In summary, the GRIAL strategy has afforded many benefits for *N*-glycan quantitation. As a preliminary report, however, further improvements for GRIAL can be as follows: first, although two isotope-coded amino acids were used, GRIAL can be readily extended to three-plex tags with (Arg^0, Arg^6 and Arg^{10}); second, using the GRIAL strategy, the loss of sialic acid was sometimes inevitable in the positive mode by using MALDI-MS (Fig. S11A, ESI†) and this phenomenon was also observed in the previous report.[17] However, this issue could be addressed by analysis of sialylated glycans in the negative mode using the GRIAL strategy (Fig. S11B, ESI†); moreover, in combination with multiple well-established chromatographic separations, GRIAL could be applied to quantify more glycans in the complex sample. Nevertheless, we have a reason to believe that GRIAL would still be a promising strategy in quantitative *N*-glycomics for the endeavor of serum biomarker discovery.

This work was supported by NST (2012CB910602 and 2012AA020203), NSF (21025519, 21335002, and 21375026), the PhD Programs Foundation of the Ministry of Education of China (20130071110034) and the Shanghai Projects (Eastern Scholar, 11XD1400800 and B109).

Notes and references

1 (*a*) H. B. Guo, I. Lee, M. Kamar, S. K. Akiyama and M. Pierce, *Cancer Res.*, 2002, **62**, 6837–6845; (*b*) K. Ohtsubo and J. D. Marth, *Cell*, 2006, **126**, 855–867.
2 (*a*) H. Ito, A. Kuno, H. Sawaki, M. Sogabe, H. Ozaki, Y. Tanaka, M. Mizokami, J. Shoda, T. Angata, T. Sato, J. Hirabayashi, Y. Ikehara and H. Narimatsu, *J. Proteome Res.*, 2009, **8**, 1358–1367; (*b*) M. J. Kailemia, L. R. Ruhaak, C. B. Lebrilla and I. J. Amster, *Anal. Chem.*, 2014, **86**, 196–212; (*c*) Y. Mechref, Y. Hu, J. L. Desantos-Garcia, A. Hussein and H. Tang, *Mol. Cell. Proteomics*, 2013, **12**, 874–884; (*d*) W. R. Alley Jr., B. F. Mann and M. V. Novotny, *Chem. Rev.*, 2013, **113**, 2668–2732.
3 W. Zhang, H. Wang, H. L. Tang and P. Y. Yang, *Anal. Chem.*, 2011, **83**, 4975–4981.
4 R. Orlando, J.-M. Lim, J. A. Atwood, P. M. Angel, M. Fang, K. Aoki, G. Alvarez-Manilla, K. W. Moremen, W. S. York, M. Tiemeyer, M. Pierce, S. Dalton and L. Wells, *J. Proteome Res.*, 2009, **8**, 3816–3823.
5 N. Hashii, N. Kawasaki, S. Itoh, Y. Nakajima, T. Kawanishi and T. Yamaguchi, *Immunology*, 2009, **126**, 336–345.

6 H. Zhou, P. G. Warren, J. W. Froehlich and R. S. Lee, *Anal. Chem.*, 2014, **86**, 6277–6284.
7 (*a*) G. Ridlova, J. C. Mortimer, S. L. Maslen, P. Dupree and E. Stephens, *Rapid Commun. Mass Spectrom.*, 2008, **22**, 2723–2730; (*b*) B. Xia, C. L. Feasley, G. P. Sachdev, D. F. Smith and R. D. Cummings, *Anal. Biochem.*, 2009, **387**, 162–170.
8 S. H. Walker, J. Budhathoki-Uprety, B. M. Novak and D. C. Muddiman, *Anal. Chem.*, 2011, **83**, 6738–6745.
9 M. J. Bowman and J. Zaia, *Anal. Chem.*, 2007, **79**, 5777–5784.
10 S. Yang, W. Yuan, W. Yang, J. Zhou, R. Harlan, J. Edwards, S. Li and H. Zhang, *Anal. Chem.*, 2013, **85**, 8188–8195.
11 H. Hahne, P. Neubert, K. Kuhn, C. Etienne, R. Bomgarden, J. C. Rogers and B. Kuster, *Anal. Chem.*, 2012, **84**, 3716–3724.
12 (*a*) X. Chen, L. Sun, Y. Yu, Y. Xue and P. Y. Yang, *Expert Rev. Proteomics*, 2007, **4**, 25–37; (*b*) Y. B. Pan, M. L. Ye, H. Zheng, K. Cheng, Z. Sun, F. J. Liu, J. Liu, K. Y. Wang, H. Q. Qin and H. F. Zou, *Anal. Chem.*, 2014, **86**, 1170–1177.
13 M. B. Liu, L. J. Zhang, L. Zhang, J. Yao, P. Y. Yang and H. J. Lu, *Anal. Chem.*, 2013, **85**, 10745–10753.
14 S. Wickramaratne, S. Mukherjee, P. W. Villalta, O. D. Schärer and N. Y. Tretyakova, *Bioconjugate Chem.*, 2013, **24**, 1496–1506.
15 J. S. Gao, D. A. Thomas, C. H. Sohn and J. L. Beauchamp, *J. Am. Chem. Soc.*, 2013, **135**, 10684–10692.
16 (*a*) H. J. An, S. R. Kronewitter, M. L. de Leoz and C. B. Lebrilla, *Curr. Opin. Chem. Biol.*, 2009, **13**, 601–607; (*b*) Y. Qiu, T. H. Patwa, L. Xu, K. Shedden, D. E. Misek, M. Tuck, G. Jin, M. T. Ruffin, D. K. Turgeon, S. Synal, R. Bresalier, N. Marcon, D. E. Brenner and D. M. Lubman, *J. Proteome Res.*, 2008, **7**, 1693–1703.
17 H. Nie, Y. Li and X. L. Sun, *J. Proteomics*, 2012, **75**, 3098–3112.